

Application of airborne LiDAR to investigate rates of recession in rocky coast environments

Claire S. Earlie · Gerd Masselink · Paul E. Russell · Robin K. Shail

Received: 30 April 2014 / Revised: 12 September 2014 / Accepted: 15 September 2014 / Published online: 1 October 2014
© Springer Science+Business Media Dordrecht 2014

Abstract Coastal cliff erosion is a widespread problem that threatens property and infrastructure along many of the world's coastlines. Rates of erosion used for shoreline management are generally based on analysis of historic maps and aerial photographs which, in rocky coast environments, does not wholly capture the detail in the processes and the failures occurring across the cliff face. This study uses airborne LiDAR (Light Detection and Ranging) data to gain a quantitative understanding of cliff erosion along rocky coastline where recession rates are relatively low (c. 0.1 m yr^{-1}).

It was found that three-dimensional volumetric changes on the cliff face and linear rates of retreat can be reliably calculated from consecutive digital elevation models (DEMs) several years apart. Furthermore, the accuracy of the data on sloping surfaces was tested by applying a threshold below which data that could be construed as error were removed. Using a vertical change threshold of 0.5 m had limited effect on the computed rates of retreat. The spatial variability in recession rates around the coastline was considered in terms of the relationship with the varying boundary conditions (rock mass characteristics, cliff geometries, beach morphology) and forcing parameters (wave climate and wave exposure). Recession rates were statistically correlated with significant

wave height (H_s), rock mass characteristics (GSI) and the ratio between the two (GSI/H_s).

The current method of assessing rocky cliff recession using maps and aerial photographs tends to not only miss the detail in the three-dimensional nature of the cliff evolution, but may also be too coarse a resolution to capture the small scale changes that contribute to the overall failure. LiDAR data, although limited in its temporal extent due to it being a relatively new technology, is a suitable method of evaluating cliff erosion on a time scale of 3–4 years and provides additional insight into the process occurring in slowly eroding environments.

Keywords Cliff erosion · Airborne LiDAR · Rocky coastlines · Digital elevation model

Introduction

Cliff erosion and the associated risks to coastal properties has been a topic of investigation for many decades; however, in the context of climate change, sea-level rise and the potential for increased storminess, the majority of coastal morphological literature has tended to focus on depositional, rather than erosive coasts (Stephenson 2006; Naylor et al. 2010). The vulnerability of different coasts can be characterised by the response to and the relaxation times between return intervals of extreme events (Pethick and Crooks 2000). In this respect, cliffed coastlines are highly vulnerable as their erosive nature makes them non-recoverable. Naylor et al. (2010) identified a significant difference between the amount of research carried out on erosive compared to depositional coasts over the last 20 years, leading to a limited understanding of the vulnerability of rocky coastlines. In particular, this refers not only to rocky coastlines alone, but also erosive coastlines with complex morphologies, such as cliffs fronted by beaches or shore

C. S. Earlie (✉) · G. Masselink · P. E. Russell
School of Marine Science and Engineering, Plymouth University,
Drake Circus, Plymouth PL4 8AA, UK
e-mail: claire.earlie@plymouth.ac.uk

G. Masselink
e-mail: g.masselink@plymouth.ac.uk

P. E. Russell
e-mail: p.russell@plymouth.ac.uk

R. K. Shail
Camborne School of Mines, University of Exeter, Penryn,
Cornwall TR10 9EZ, UK
e-mail: R.K.Shail@exeter.ac.uk

platforms, and composite cliffs that vary in hardness throughout their vertical profile (Naylor et al. 2010). In this paper, the relative resistance of rocks is characterised by the lithology of the rock as well as the rock mass characteristics that control the intrinsic resistance to erosion. The majority of cliff erosion studies in the UK have focused along the eastern and southeast coast of the country due to the very high rates of recession that are a consequence of the ‘soft rock’ geology (till, chalk, clays and heavily weathered shales) (Hall et al. 2002; Damgaard and Dong 2004; Dong and Guzzetti 2005; Lee 2008; Dawson et al. 2009; Brooks and Spencer 2010; Ashton et al. 2011; Brooks et al. 2012). Both in the UK and globally, limited literature exists on the evolution of harder rock coastlines and their response to coastal erosion. Here we refer to ‘hard’ rock geology as comparatively more resistant and lesser weathered sandstones, mudstones, shales and granite.

The widespread problem of cliff erosion and the sustainable management of this risk require robust quantification of erosion rates, but these are often difficult to obtain along rocky coasts using current methods. Cliff erosion studies have typically involved historic mapping, photogrammetry or terrestrial laser scanning to determine cliff face volumetric changes and rates of retreat. Rates of erosion in rocky coastlines found using these techniques range from 0.02 to 0.5 m yr⁻¹ (Rosser et al. 2005; Ridgewell and Walkden 2009; Lim et al. 2010). The variation in these rates depends largely on the geological characteristics, wave exposure and meteorology. The spatial and temporal variations in the type of analysis technique will also influence the resultant rate of erosion, and hence the interpreted amount of vulnerability, due to the resolution of data capture in the method itself.

In shoreline management strategies, historic shorelines are digitised and recession rates calculated using the ArcGIS Digital Shoreline Analyst Software (DSAS) tool (Ridgewell and Walkden 2009; USGS 2012). The site-specific detail is missed using this method as the rates are summarised on a larger scale (10’s–100’s km) and, for the purposes of policy formulation and development, only the cliff top position is considered. The nature of rocky coastlines and the modes in which failure occurs (often on the cliff face) calls for a more detailed understanding of the way in which the cliffs behave (Rogers et al. 2009). With advances in technology, the three-dimensional nature of the evolution of cliffs has become easier to capture. Terrestrial Laser Scanning (TLS) or photogrammetry are both methods that allow for very high resolution georeferenced data to be obtained for cliff faces (Rosser et al. 2005; Young et al. 2009; Dewez et al. 2013). However, there are often issues with photogrammetry regarding accuracy (Adams and Chandler 2002). TLS is useful for more site-specific and localised changes (10–100 m), yet such methods may not be feasible in some difficult to reach locations.

Airborne LiDAR (Light Detection and Ranging) has been used as an accurate and reliable method of obtaining

georeferenced geospatial data since the 1980s (Adams and Chandler 2002; Young and Ashford 2006; Brock and Purkis 2009; Young et al. 2009; Lim et al. 2011; Nunes et al. 2011; Young et al. 2011a) and has proven to be useful for determining volumetric changes in a variety of coastal landscapes. Large scale data sets can be obtained at a high spatial resolution (0.5 m²) and repetitive annual surveys can be compared and used to assess coastal erosion. LiDAR has been used extensively for fluvial and coastal flood risk assessment over the last decade (Geomatics Group 2012). The method is often used to assess sediment budgets and pathways for coastal defence construction, and for existing and future coastal developments all over the world (Sallenger et al. 2003; Zhang et al. 2005; Xhardé et al. 2006; Young and Ashford 2006; Brooks and Spencer 2010; Nunes et al. 2011; Schmidt et al. 2011; Young et al. 2011b; Jaboyedoff et al. 2012). The high resolution of LiDAR (footprint of 0.5 m²) means that in coastal slopes and non-vertical cliffs, the face of the cliff can be surveyed and changes occurring on the cliff face can be captured. The coast of California, for instance, is frequently surveyed and monitored due to the high levels of coastal erosion and the high value of properties at risk. Here, airborne LiDAR has successfully been used to assess volumetric changes to the cliff face and sediment inputs into the nearshore (Young and Ashford 2006; Young et al. 2009; 2011a; 2011b), and also to determine localised cliff recession rates (c. 0.03–0.13 m yr⁻¹).

The public availability of LiDAR data makes this an ideal method of assessing coastal change at a range of spatial scales, from metres to tens or hundreds of kilometres. LiDAR data also enables the assessment of coastal change at inaccessible/unsafe regions. This study uses LiDAR data from two different periods (2007/2008 and 2010/2011) to derive rates of retreat from volumetric changes to the cliff face, top and toe at 10 coastal sites in the south-west of England. Firstly, we aim to quantify the spatial variability of coastal cliff erosion at these different sites, which are located around a lithologically resistant, highly energetic coastline with three different coastal orientations. These rates are also considered in terms of their relationships with the spatial variability in boundary conditions and forcing parameters (rock mass characteristics and wave climate). Secondly, we will compare these annual cliff retreat rates to the annual rates obtained from longer time periods used for shoreline management purposes to evaluate whether short-term LiDAR data can be used as a suitable method to estimate long-term cliff recession along rocky cliffed coastlines.

Study area

Cornwall forms the south-west peninsular of the UK and this 525-km long coastline that protrudes into the Atlantic is subjected to a highly energetic wave climate (Scott et al.

2011). The variability in geology and the spatial differences in the resistance of rock to erosion (Bird 1998) means that the region experiences localised elevated rates of erosion ('hot spots') that are a result of a combination of episodic failures (Cosgrove et al. 1998) and gradual erosion over the longer term (Shail et al. 1998). Ten sites were selected to represent a range of rock mass characteristics and varying wave exposures (Fig. 1). These sites, which are all owned by the National Trust (a UK conservation charity who protect historic land and property), were also identified as having particularly pressing issues with coastal erosion.

Geological setting

Geologically, the coast is dominated by metasedimentary rocks developed during the Devonian to Carboniferous rifting. The deformation of rocks during the Variscan Orogeny and the horizontal stresses exerted on the rocks led to the folding, faulting, thrusting and regional low grade metamorphism noted in the exposed cliffs along the coast. Following this period, these rocks were all cut by a variably reactivated network of Carboniferous-Triassic faults, formed as a result of the vertical pressures applied during the late Carboniferous. It is the structure, orientation, spacing and frequency of these discontinuities that ultimately determine the resistance of the rocks to erosion (Leveridge and Hartley 2006; Leveridge and Shail 2011).

All sites are situated on sedimentary/metasedimentary bedrock, with the exception of Porthcurno on Land's End peninsular, which is a granite outcrop. Nearly all of the sites, including Bedruthan Steps, Trevellas Cove, Portreath and Godrevy on the north coast, and Porthleven and Church Cove on the south coast, are characterised by Lower Devonian lithology comprising medium to coarse-grained sandstones or dark grey mudstones/shales interbedded with fine-grained silty sandstones. The Porthleven site incorporates an additional site, Caca Stull Zawn, which is a shore-perpendicular thrust fault formed as a result of deformation processes during the Variscan Orogeny (Leveridge and Shail 2011). Porthcurno on the south coast is an igneous intrusion, a granite headland from the Permian/Carboniferous age. Pendower, Hemmick and Seaton, all on the south coast, are characterised by Upper, Middle and Lower Devonian lithology with fine to medium sandstones or mudstones/shales interbedded with coarse sandstones (Shail et al. 1998; Westgate et al. 2003; Leveridge and Hartley 2006). Most of the sites are formed of two geological units, with Carboniferous to Devonian bedrock overlain by a layer of superficial Quaternary deposit (poorly consolidated periglacial sedimentary head deposits comprising clay, silt, sand and gravel), the thickness of which varies around the coast from 0 to 15 m (Shail et al. 1998; Westgate et al. 2003).

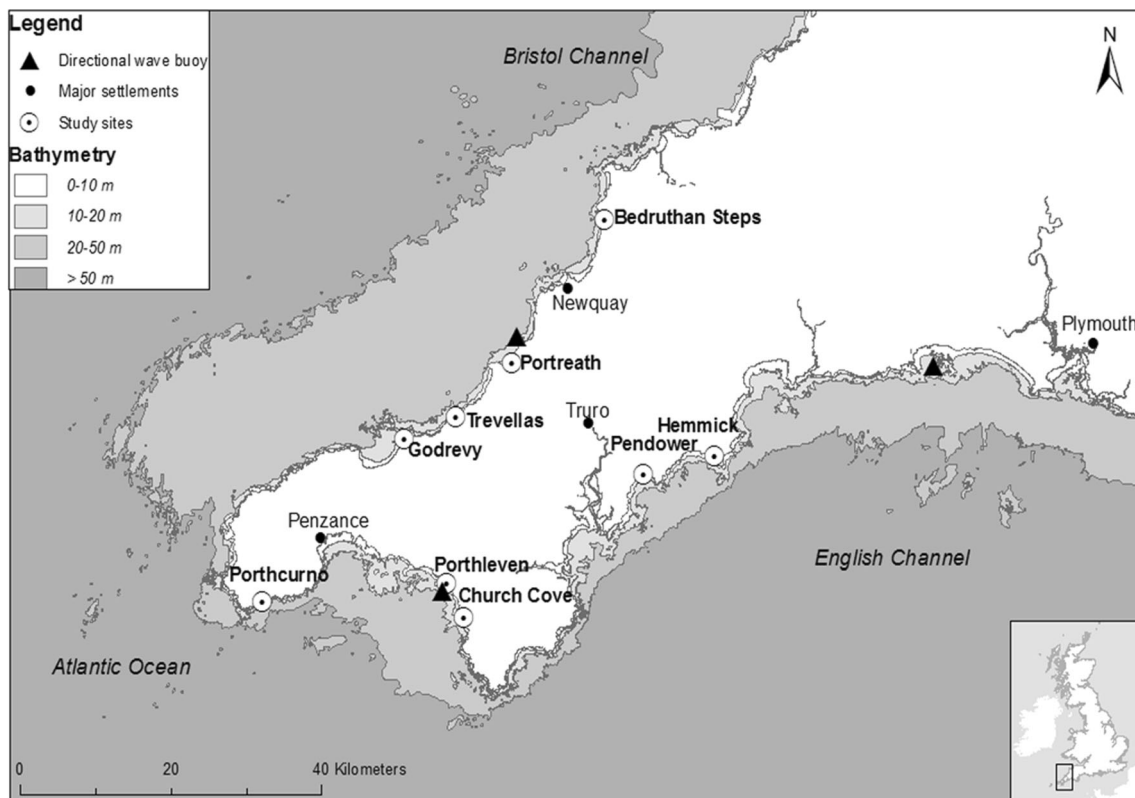


Fig. 1 Locations of the study sites around the south-west peninsular of the UK and the wave buoys used to determine regional wave climate

Wave climate

The wave climate around the Cornish coastline is the most energetic of UK coastal waters (Scott et al. 2011). The north coast is exposed to high energy swell waves from the Atlantic Ocean and wind waves generated by the prevailing westerly winds. The south-west coast receives wind waves from the south-west and less frequent swell, whilst the sites further to the east, along the south-east facing coast (Fig. 1) mainly receive wind driven waves from the English Channel. Therefore, the three different coastal orientations experience a varying wave climate. All Cornwall's beaches are macrotidal with spring tidal ranges varying around the coast from 4 to 4.8 m along the south and south-west coasts, and between 5.5 and 6.4 m along the north coast (UKHO 2012).

Climate

The climate of Cornwall is influenced by temperate maritime air with average temperatures of 9–11 °C and a regional annual rainfall total of 900–1,100 mm. Temperatures that are cold enough to bring ground frost are only found 15–20 days out of the year and are rarely found at sea level (Met Office 2012). Annual rainfall totals show little variability around the Cornish coastline; therefore, any spatial variability in erosion rates is unlikely to be attributed to differing weather conditions around the coast.

Method

Quantification of geological parameters

Typical methods of quantifying the rock mass strength characteristics include statistically analysing results from multiple tri-axial tests on core samples or using a Schmidt hammer to determine the compressive strength of a rock sample (Wyllie and Mah 2004). In rocky coastal environments, studies have highlighted how it is primarily the intrinsic structural controls on the rock mass that ultimately determine its vulnerability to erosion more than the compressive strength of the rock itself (Shail et al. 1998; Wyllie and Mah 2004; Dornbusch and Robinson 2005). The spacing, frequency and orientation of the principal discontinuities that formed during the post-Variscan deformation towards the Upper Carboniferous (Shail et al. 1998), as well as the subsequent joints and cleavages within the rock, are all important for dictating the potential for cliff failure and the mechanism via which it may occur. The Geological Strength Index (GSI) classification proposed by Hoek et al. (1998) is a method of quantifying the rock mass strength and deformability parameters based on a visual impression of the rock structure. It allows an assessment of the

condition of the rock surface based on the extent of weathering apparent and the level of alteration the surface of the rock has undergone. The classification scheme also considers the spacing, frequency, roughness and orientation of the visible discontinuities to determine the kinematic stability of the rock (Wyllie and Mah 2004). The GSI produces high value (100–70) for rocks that have an unweathered or unaltered surface condition and a well interlocked rock mass with few discontinuities and a low (0–20) GSI value for highly weathered, heavily broken rock mass with numerous poorly interlocked discontinuities. As it was not possible to obtain core samples for tri axial testing or carry out extensive in-situ kinematic analysis, rock mass characteristics obtained from field observations were applied to the GSI method as a simplified means of determining the relative strength of the bedrock at each site (Table 1).

Wave climate analysis

Cliff erosion studies have previously focused on the following cliff failure factors: rainfall, strength of rock, rock mass characteristics and slope stability. Aside from the general understanding that waves tend to weaken the cliff at the toe and remove the protective talus material, only recently has research been directed towards linking the potential for weakening of the rock mass structure with exposure to waves (Adams and Chandler 2002; Adams et al. 2005; Young et al. 2009; Young et al. 2011a; Dickson and Pentney 2012; Lim et al. 2011). It was not possible in this study to compare a time series of wave climate with cliff failure as the time period between consecutive LiDAR flights is too long to identify individual failures with a particular event. However, the relation between the spatial variability in erosion rates and that of the wave exposure around the south-west peninsular is worth considering.



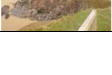
A SWAN regional wave model for the south-west peninsular of the UK, provided hindcasted wave statistics for the study area (Fig. 2). The model outputs significant wave height (H_s), peak spectral wave period (T_p) and wave direction (θ) (Austin et al. 2013) every 30 min, with data for a 3-year period statistically analysed. These values were used to determine the percentage occurrence statistics for wave heights and periods from different directions. The purpose of using these data is to characterise the nearshore wave climate at each of the sites and determine the variability in energy that is delivered to the cliffs around the coast.

Rocky coast evolution model

Rock coast evolution is typically understood to be a function of wave height, and relative rock strength, as proposed by Sunamura's rocky coast evolution model (1992).

$$\frac{Sc}{\rho g H_1} \quad (1a)$$

Table 1 Characteristics of the study sites. Average cliff height determined from LiDAR data; lithology taken from Ridgewell and Walkden (2009); and failure information based on Bird (1998), Orford et al. (2002) and Leveridge and Shail (2011). GSI values calculated from recent (2012) field observations

Location	Average Cliff height (m)	Lithology	GSI	Failure Mechanism	Activity	Recession Potential (m yr ⁻¹)	Image
Hemmick	11	Hard sandstones and mudstones with some superficial deposits, cliffs (Dodman Phyllites) thrust over Pendower Formation (brecciated slates and limestones with igneous intrusions)	55-58	Mainly rotational failure of superficial material, block removal or planar failure unlikely. Debris slides and rockfalls possible	Inactive	<0.1	
Pendower	20	Superficial head deposits above emerged beach, above emerged shore platform, above Pendower formation bedrock	37-40	Undercutting, some block removal and collapsing, low potential for planar failure or slippage	Inactive	0.1 – 0.5	
Church Cove	20	Sandstones and mudstones overlain by head deposits	30-35	Block removal, of toe material and wedge and planar failure of upper cliff material. Topples occurring in superficial deposits	Inactive	<0.1	
Porthleven	5-25	Sedimentary gramscatho beds with interbedded slates and sandstones. Mylor slates overlain by head of clay, silt, sand and gravel. Porthleven cliffs are SSSI, Devonian sediments with basaltic intrusions	25-30	Mainly block removal, and wedge failure leading to slumping or collapse of superficial material. Block removal in fault (Caca stull Zawn) leads to toppling and planar failure	Inactive	<0.1	
Porthcurno	50	Mostly granite	70-75	Block removal rarely, some topples and rockfalls	Inactive	<0.1	
Godrevy	15	Rubbly head, varying from 3-8 m over pebbly emerged beach, sitting upon Pleistocene emerged shore platform, cutting over Porthtown slates with interbedded sandstones	40-50	Block removal of bedrock and toppling leading to slumping or rotational failure of superficial deposits. Also terrestrial processes leading to slumping of head	Active	0.1 – 0.5	
Portreath	25	Porthtown formation slate with mudstones and sandstones	45-50	Failures look more fault controlled than block removal, orientation of discontinuities suggests toppling failures or undercutting within faults leads to collapse	Active	0.1 – 0.5	
Trevellas	50	Metasedimentary Devonian slate with sandstones and limestones some superficial deposits	33-36	Block removal at the toe of the cliffs have led to material above translating down the cliff slope. Rotational sliding and slipping apparent in superficial material	Active	<0.1	
Bedruthan Steps	50	Large exposed slate outcrops on the beach, cliffs are grey and green slates with limestone bands some head	30-34	Block removal of lower material leading to rotational sliding of upper cliff, rockfalls, topples and slipping apparent	Active	0.1 – 0.5	

Where S_c represents the resisting forces (compressive strength of the cliff material) and $\rho g H_1$ represents the assailing forces (where ρ is the density of water, g is the gravitational acceleration and H_1 the height of the largest waves in the area under consideration) (Sunamura 1992). Five wave breaking scenarios are considered in Sunamura's model, and rock strength is qualitatively categorised into three categories; very strong, moderately strong and weak. Although it assumes the rocks are insoluble and uniform, and no sediment accumulation takes place in the nearshore, Sunamura's model is applicable in the rocky coast environment as it effectively captures the relationship between the boundary conditions (rock strength) and forcing (wave climate). In our study, GSI was substituted for compressive rock strength in order to account for the discontinuities and rock mass characteristics and the significant wave height (H_s), to represent the wave climate (Eq. 1b).

$$\frac{GSI}{H_s} \quad (1b)$$

LiDAR data collection and analysis

LiDAR surveys were carried out by the Environment Agency Geomatics group and provided in raster format by the Channel Coastal Observatory (CCO 2012). LiDAR data were obtained

for each site for 2007/2008 and 2010/2011, providing a c. 3-year period within which to analyse any change. The surveys are carried out over the UK coastline annually; however, only certain sections of the coast are flown each year and therefore it was not possible to compare all sites within the exact same time frame. For the purpose of this study this is not an issue as we are attempting to understand the variability in recession rates on a larger spatial scale and not relate failure events to each other or individual storm events. Intermediate values are not available for these sites as there is no current method of continual monitoring. Apart from the long term rates in the Shoreline Management Plan (SMP2) (Ridgewell and Walkden 2009), LiDAR data are the only easily accessible means of assessing the evolution of the Cornish coastline.

The LiDAR data, checked against the aircraft trajectory using the Global Navigation Satellite System (GNSS), were smoothed to output a georeferenced point cloud. Alongside the LiDAR flights, RTK dGPS surveys were undertaken over a paved unchanged surface and used to ground truth the LiDAR data (Geomatics Group 2012). A bare earth Digital Elevation Model (DEM) was generated by passing the point cloud data through classification routines and interpolated using specialist software (Geomatics Group 2012). A ground truth check was repeated, the Root Mean Squared Error (RMSE) calculated and the DEMs edited to provide a more realistic bare earth. Last returns were used here as they

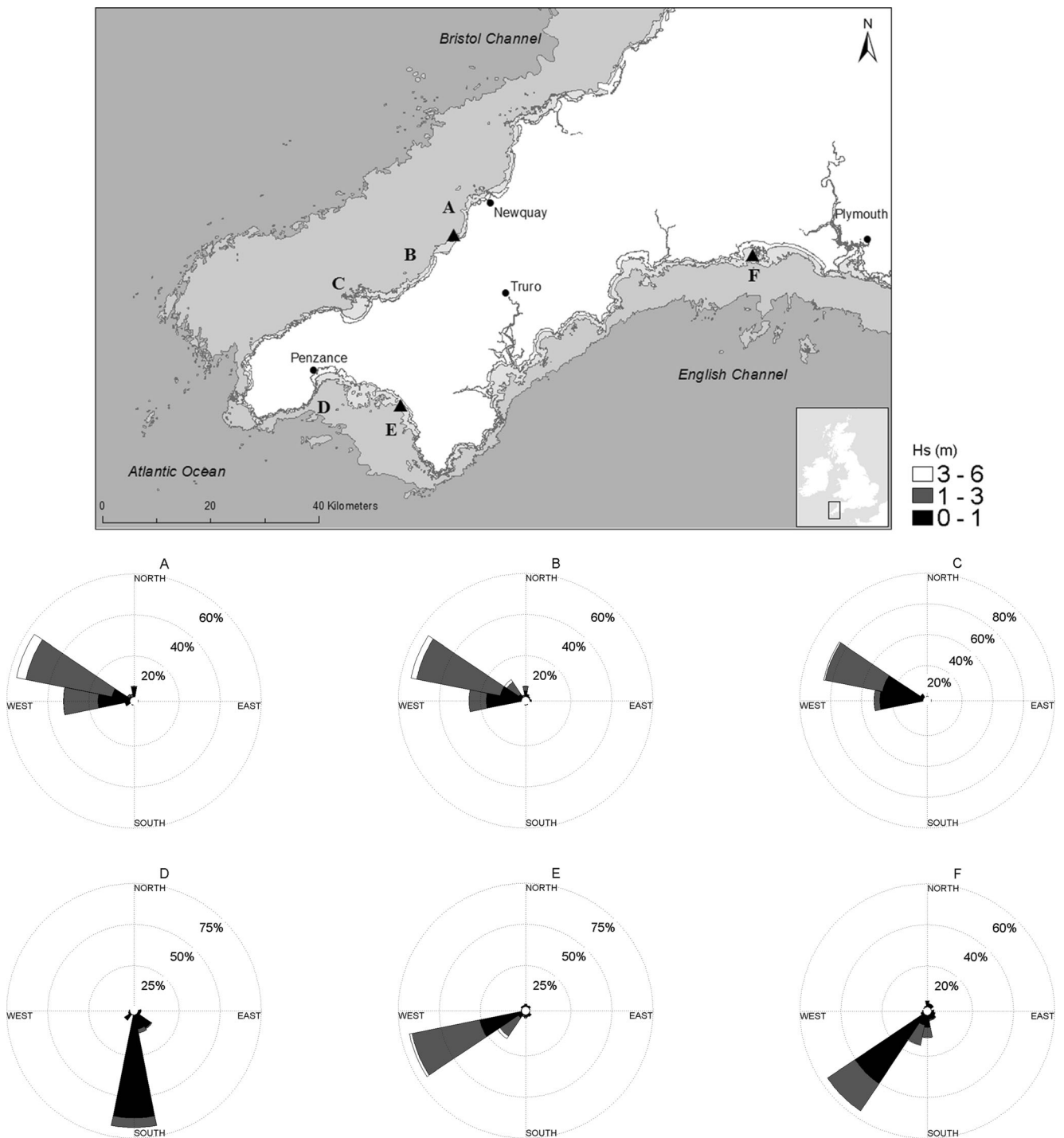


Fig. 2 Wave climate around the coastline, derived from SWAN wave model data (Austin et al. 2013). Roses represent percentage occurrence statistics for H_s from different directions at various nodes around the

coastline. Nearest nodes for each site; **a** for Bedruthan Steps, **b** for Trevellas and Portreath, **c** Godrevy and, **d** for Porthcurno, **e** for Porthleven and Church Cove, **f** for Hemmick and Pendower

produce the most accurate bare earth DEMs (Kidner et al. 2004; Leigh et al. 2009; Hladik and Alber 2012). Once removed of error and any vegetation filtered, the data are provided to the Channel Coastal Observatory in georeferenced raster format and published for use in geographical information software (CCO 2012). Difference plots were obtained by

comparing two LiDAR data sets, converted into Digital Elevation models (DEM) in ArcGIS 10 (ESRI 2011), and subtracting 1 year from another (Fig. 3). The purpose of this was to be able to ‘mask’ the cliff data, the cliff toe and the cliff top, so volume differences unrelated to cliff processes (e.g., due to beach change) could be excluded, and only changes to

the cliff toe, face and top were considered. The masked regions were converted into ASCII format, to be exported for analysis. With information of the cliff surface area and the time period between the two LiDAR flights, the rate of retreat was calculated using the following equation:

$$R = \frac{V}{Z_c L_c T_c} \quad (2)$$

Where R =linear rate of retreat (m yr^{-1}), V =net volumetric erosion (m^3), Z_c =average cliff height (m), L_c =longshore length of cliff (m) and T_c =time interval between consecutive surveys (yrs) (Young et al. 2006).

The DEM of difference plots allowed for both a quantitative and qualitative view of the changes occurring to the cliff face. Cliff profiles were interpolated along the face of the cliff to provide a visualisation of the failure mechanisms occurring at the difference sites (Fig. 3). Frequency distribution plots provide information on the varying magnitudes of change detected at each site.

An important parameter to consider with respect to the various processes occurring at each site was the frequency and extent of inundation of the cliffs to the waves. The exposure of the toe of the cliff (Z_b) was determined at each site from the LiDAR data, where elevation of the beach relative to the toe of the cliff was compared with mean sea levels.

The errors associated with using LiDAR (Zhang et al. 2005) call for removal of data below a certain threshold to determine accurate magnitudes of change. A sensitivity analysis exercise was carried out for the same sites (Earlie et al. 2013) to derive appropriate thresholds to eliminate data which could be attributed to error.

Results

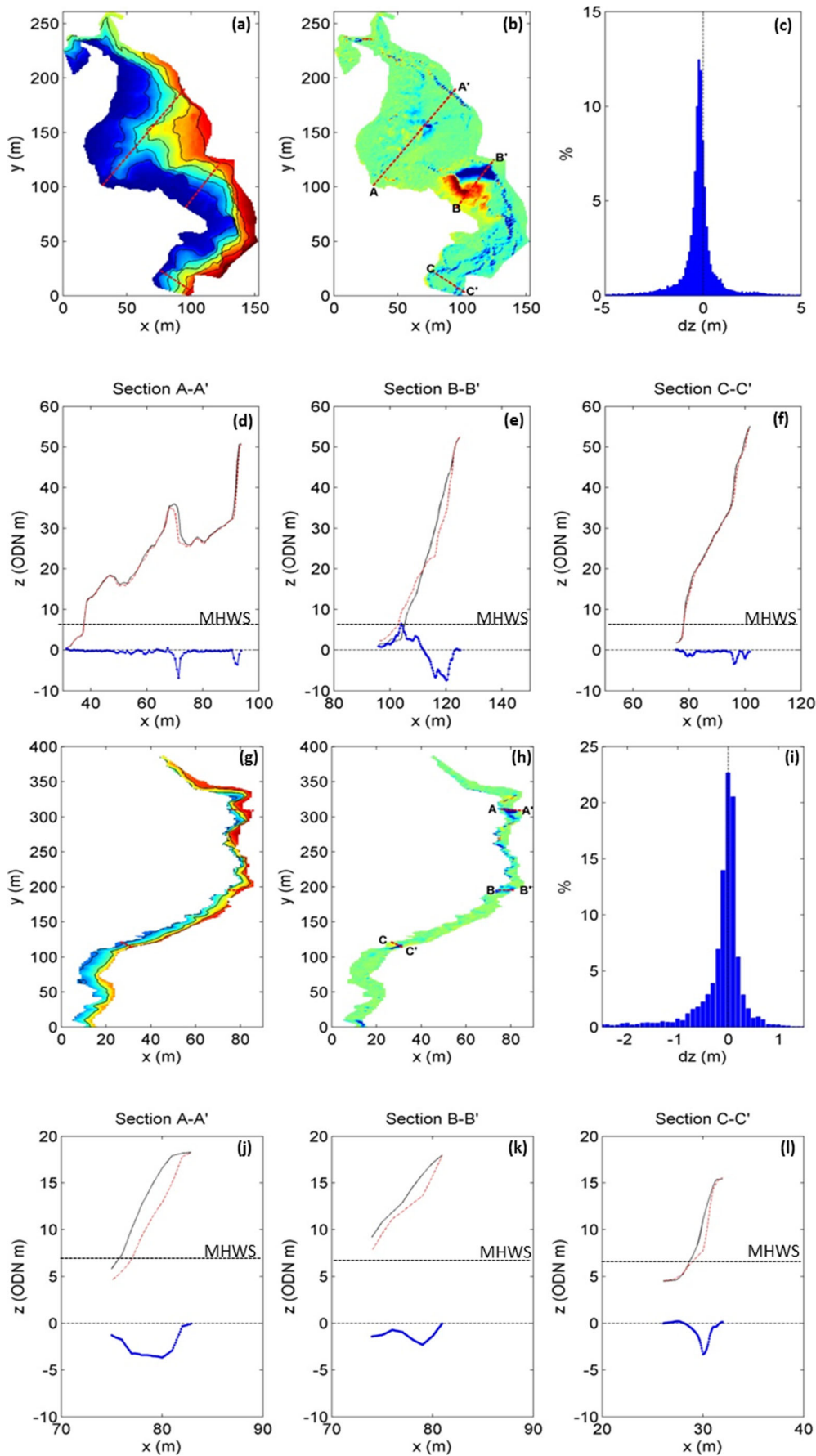
Rock mass characteristics

Cliff failure or mass wasting tends to occur through different mechanisms, according to the rock mass characteristics and principal discontinuities (Section 3.1). Typical failure mechanisms noted around the Cornish coastline are varied and range from translational (planar or wedge failure), rotational to toppling and rockfalls (Shail et al. 1998; Westgate et al. 2003; Leveridge and Hartley 2006). Alongside terrestrial processes leading to slumping of superficial material, wave-induced block removal at the toe of the cliffs tends to be apparent at all of the sites. A summary of the geology, failure mechanisms and coastal recession potential, based on site visits and a national shoreline behavioural study carried out

by Orford et al. (2002) for each stretch of coast is presented in Table 1. What is interesting to note is how the sites are identified as active or inactive according to their recession potential values ($<0.1 \text{ m yr}^{-1}$ for 5 of the 9 sites and $0.1\text{--}0.5 \text{ m yr}^{-1}$ for 4 out of the 9 sites). The GSI values identified from recent field observations in this study provide additional detail of the potential for recession, suggesting that the cliff surfaces exposed at sites have a much lower rock mass strength at Porthleven (25–30), Bedruthan Steps (30–34) and Trevellas (33–36) compared to Hemmick (55–58) and Porthcurno (70–75) (Table 1).

Waves, tides and beach morphology

Wave rose diagrams for the mean significant wave height H_s indicate the SWAN output at certain nodes around the coastline (Fig. 2). The north coast experiences a spatially-varying mean significant wave height ranging from 1 m for the north-facing (more sheltered) stretches of coast and 1.42 m along the more exposed west and north-west regions, with 10 % of the waves during this period exceeding 2–3 m at all three nodes. Statistics for the south-west coast showed a mean H_s of 1.33 m, with 10 % of the waves exceeding 2–3 m, and the south-facing coast is a less energetic, with a mean H_s of 0.87 m and a 10 % exceedance H_s of 1–2 m. The peak wave periods tend to average 9 s for the north and south-west coast, and 5 s on the south coast. The maximum wave period reaches a maximum of 16 s around the whole coastline. For some sites, (e.g., Porthcurno), wave climate is determined from the Loe Bar node (Fig. 2). This is because the nearest node (Penzance) is situated in a sheltered region and would not accurately represent the wave climate in Porthcurno. We would, however, expect to see a slightly less energetic wave climate than depicted by the Loe Bar node, because Porthcurno is south facing and is therefore, slightly more sheltered. Therefore an average between the Loe Bar and Loo Bay node has been used to characterise the wave climate here. The exposure of the cliffs to the waves and the vertical run up extent will vary locally and seasonally according to the tidal range, beach morphology, surge and significant wave height. The local tidal ranges and mean beach/cliff junctions presented in Table 2 provide a general indication of the extent of tidal inundation of the cliffs. The greatest tidal ranges are seen on the north coast with mean spring ranges in the region of 6 m. The coincidence of the tidal levels with the cliff toe will depend on the beach elevation and beach morphology. The sites that experience the greatest water inundation in terms of still water levels in relation to beach/ cliff junction levels are Bedruthan Steps, Porthcurno and Trevellas, and the least ‘exposed’ sites are Porthleven, Godrevy and Hemmick.



◀ **Fig. 3** DEMs, frequency distributions and cross-shore profiles for Bedruthan Steps (3a-3f) and Godrevy (3g-3l). Fig. 3a and g show contoured DEM with the *x*-axis as cross shore distance and the *y*-axis, longshore distance. Colour bar shows elevations from 0 m (blue) to 50 m (red). Fig. 3b and h are DEMs of difference, with the colour bar indicating surface change (erosion) of up to -8 m (blue) and accumulation of material (red) of up to +5 m. Frequency distributions of the percentage of vertical change (*dz*) between the 2 years are illustrated in Fig. 3c and i. The A-A', B-B' and C-C' profiles are plotted in Fig. 3d-f and 3j-l with the solid line indicating the 2008 profile and the dotted indicating the 2010/11 profile in relation to MHWS. The bold line in these plots indicates the difference in elevation between the 2 years across these profiles

DEM's of difference and rates of retreat

The DEMs of difference plots not only provide an illustrative method of highlighting active regions within the vulnerable sites, but also allow for the changes that have occurred over the time period to be quantified and erosion rates calculated (Eq. 2). Two sites have been presented here to demonstrate the capability of LiDAR data in capturing changes to the cliff face and highlight the variability in the magnitudes of failure noted around the coastline. At Bedruthan Steps, the erosion/accretion patterns along the cliff face are spatially highly variable, and, as illustrated in the large mass movement in the centre of the study area (Fig. 3; cross section B-B'), negative changes greater than 10 m in the vertical can be seen. This event is largely responsible for the large long-term recession rate deduced from these data, highlighting the sensitivity of the result on single events. In addition to the large mass movement, various smaller changes are obvious along the upper cliff edge. The cliff profile at Godrevy is much steeper (69°) than Bedruthan Steps (43°); therefore, the footprint of the DEM from the LiDAR is much narrower. Plotting profiles across the cliff, however, shows how the volume change is

Table 2 Beach/cliff elevations (obtained from LiDAR data) and tidal levels and ranges for the nearest secondary ports (UKHO 2012), and mean significant wave heights from the nearest SWAN output nodes

	Beach/Cliff elevation (m ODN)	MHWS (m ODN)	Tidal range (m)	Mean H_s (m)
Hemmick	2.7	2.4	4.7	0.87
Pendower	1.7	2.5	4.6	0.87
Church Cove	1.8	2.4	4.7	1.33
Porthleven	5.3	2.5	4.7	1.33
Caca Stull Zawn	4.4	2.5	4.7	1.33
Porthcurno	0.7	3.0	5.4	1.1
Godrevy	4.8	3.2	5.8	1.01
Portreath	3.5	3.5	6.1	1.36
Trevellas	2.7	3.5	6.1	1.36
Bedruthan steps	0.5	3.5	6.5	1.42

still captured and a net loss of material can be quantified even on steeply sloping cliff faces.

The changes to the cliff face are further illustrated in cross-shore profile lines interpolated from the DEMs where removal of material higher up the cliff face and deposition of this material lower down is apparent. Gradual erosion of material across the whole vertical profile of the cliff face is also shown in the cross-shore profiles of Godrevy and in the high percentage of smaller changes in the frequency distributions.

The highest cliffs in the study are found at Porthcurno (50 m), Trevellas (70 m) and Bedruthan Steps (45 m), and the smallest at Hemmick (11 m), Pendower (10 m) and Godrevy (15 m); the steepest cliffs are found at Porthleven (73°), Portreath (75°) and Godrevy (69°). The sizes of the regions of interest at each site (longshore length of cliff (L_c)) vary, but this does not affect the rate of retreat as this figure is based on erosion per metre of cliff. The largest volume changes during this period occurred at Bedruthan Steps (5,422 m³), Porthleven (1,374 m³), Church Cove (1,092 m³) and Trevellas (1,079 m³), with little change noted at Hemmick, Pendower and Porthcurno (all < 40 m³). With information about the area of the region of interest (H_c and L_c) and the time period between consecutive surveys (Eq. 2) (T_c), the rate of recession of the cliff (R) can be calculated (Table 3). These rates vary by an order of magnitude around the coastline, from 0 at Porthcurno to 0.37 m yr⁻¹ at Caca Stull Zawn.

Discussion

Sensitivity analysis of LiDAR

Figure 4 provides the DEMs of difference between, and the frequency distributions of the vertical surface elevation change for all ten sites. Although the coastline of the southwest of the UK is characterised as a slowly eroding coastline in comparison to the south and eastern coasts of the country, what is apparent from the plots is the variability in the magnitude of erosion that is detected using this method and is suggestive of some of the processes occurring at each site. The DEMs and the frequency distributions very clearly highlight the sites that experienced greater activity during the study period. For example, Bedruthan Steps, Porthleven, Caca Stull Zawn and Church Cove prove to be much more active (more negatively skewed distributions; meaning more losses than gains) than Pendower and Porthcurno. This suggests that there are regions where failure occurs and material remains part of the system (e.g., at Bedruthan Steps where positive and negative changes are noted), whereas at other sites material that is removed from the cliff face is removed by waves (e.g., at Godrevy and Porthleven where there distributions are more negatively skewed).

Table 3 Cliff dimensions and resultant rates of retreat obtained from LiDAR-derived DEM comparisons

	Net Volume loss (m^3) (V)	Ave cliff height (m) (H_c)	Average slope ($^\circ$)	Longshore length (m) (L_c)	Time interval (yrs) (T_c)	Rate of retreat (m yr^{-1}) (R)
Hemmick	40.37	11	68	40	3.8	-0.03
Pendower	39.66	10	66	370	3.8	-0.01
Church Cove	1091.80	20	42	64	3	-0.29
Porthleven	1373.50	17	73	265	3.5	-0.09
Caca Stull Zawn	642.00	24	60	20	3.5	-0.37
Porthcurno	0.053	50	73	780	3	0.00
Godrevy	677.83	15	69	660	2	-0.04
Portreath	623.54	26	75	135	3	-0.06
Trevellas	1078.50	70	51	200	1	-0.08
Bedruthan Steps	5422.10	45	43	380	2.5	-0.17

The accuracy of LiDAR is understood to decrease as cliff slope angle increases (Adams and Chandler 2002; Xhardé et al. 2006). It is not possible to test this notion in this situation as the only locations within the LiDAR tile that are certain to have not changed between the LiDAR surveys are on flat ground. A method of assessing whether the change seen on

sloping surfaces is actual change or error inherent in the LiDAR method, is by applying a gradually increasing threshold (0 to 10 m at 10-cm intervals) to the volume differences to remove any data that may potentially be construed as error (Wood and Fisher 1993; Earlie et al. 2013). This allows us to determine whether the net rate of retreat is influenced by this

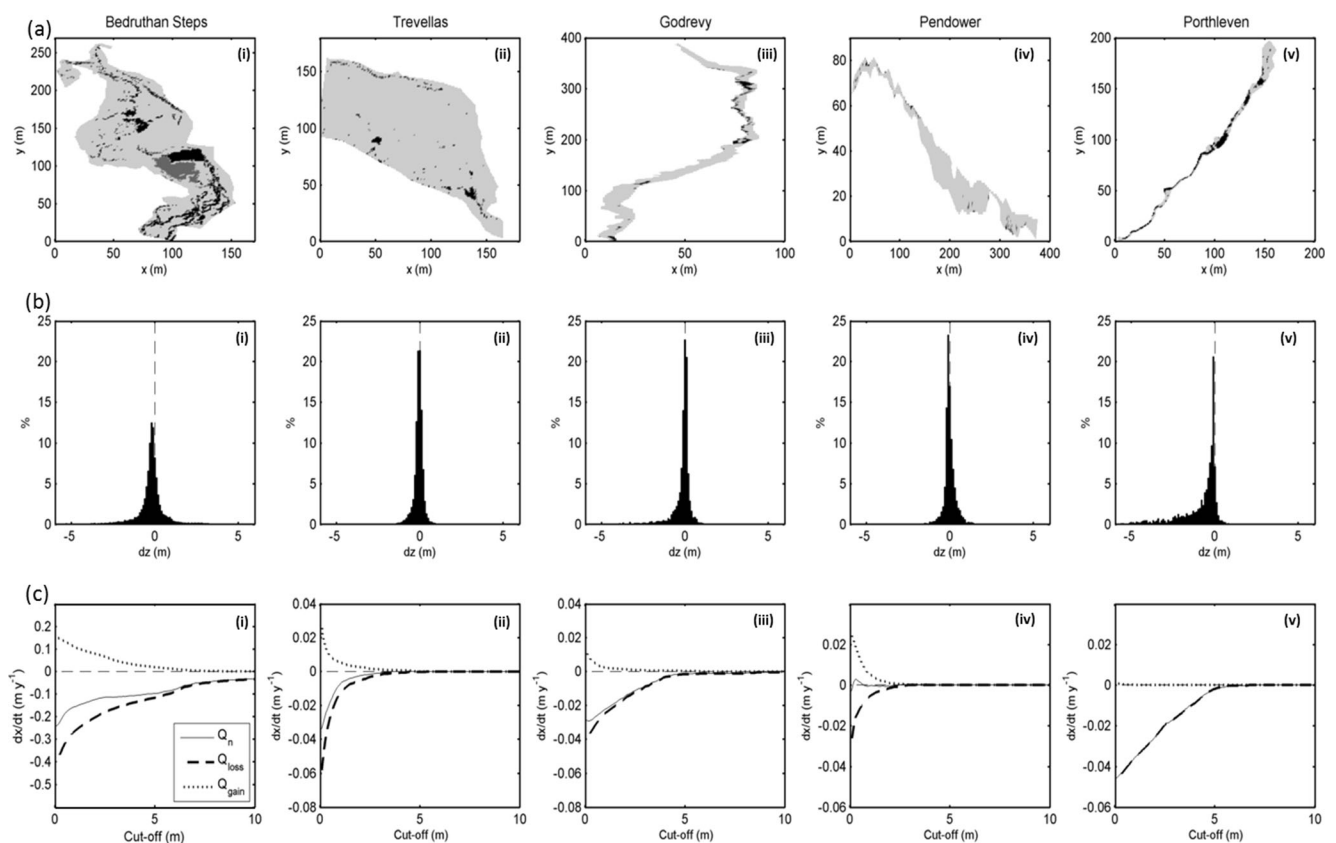


Fig. 4 a (i-v) - DEM's of difference (x -axis; cross-shore, y -axis; longshore); where *darker gray* regions represent accumulation of material, *black* regions represent erosion and *light gray* shows no change. b (i-v) - frequency distribution (vertical change, dz versus %). c (i-v) - sensitivity analysis of recession rate (x -axis) to a

gradually increasing error threshold (y -axis) for all ten sites. The small dashed line in these plots represents the total positive changes (accumulation of material), the thick dashed line represents total negative changes (erosion) and the solid line represents the net change (V)

‘cut-off’ (Fig. 4c (i-v)). This sensitivity testing allows us to assess how the resultant rate of retreat will change according to how much of the data is considered error; hence, how much valid data are eliminated (Earlie et al. 2013). Five out of the ten sites are presented here to demonstrate the sensitivity analysis process. All five plots show a decrease in net erosion with an increasing threshold. The point at which this value reaches zero varies, depending on the size of the failures noted in relation to the threshold (Fig. 4c (i-v)). What is apparent from these plots is that LiDAR is able to accurately detect failure on sloping surfaces, as even if the conservative cut-off threshold of 0.5 m is used to eliminate potential error, very little reduction in the net volume difference is seen, compared to using no threshold. Using this method allows for the smaller changes that are often difficult to detect using historic mapping or photogrammetry to be accountable for the change in volume, as well as the larger mass failures.

Physical parameters and rates of retreat

It is rare for both the geotechnical resisting forces (lithology and rock mass characteristics) and the erosive forces (tide data, wave climate) to be included in process-based cliff erosion studies (Rosser et al. 2005; Rosser et al. 2007; Naylor et al. 2010). Many investigations are site-specific and, although in this study a relatively small data set has been obtained, it represents one of the first longitudinal data sets that has been used to consider both the boundary conditions and the forcing parameters, and attempts to draw relationships between these spatially-varying parameters (Fig. 5).

What is initially apparent from Fig. 5 is that the sites along the west, north-west and south-west facing coast experience greater rates of erosion than the sites along the south-east coast, varying by almost an order of magnitude from 0.00–0.03 m yr⁻¹ to 0.05–0.37 m yr⁻¹. The more sheltered sites along the south-east coast experience smaller significant wave heights and peak wave periods than those along the north-west coast. The wave exposure values (Z_o) refer to the average elevation of the beach at the cliff toe relative to mean high water springs (MHWS). Negative values indicate that the cliff base is located above MHWS and therefore not affected by wave action over most of the tidal cycle, whereas positive values indicate that the cliff base is located below MHWS and is subjected to wave action over most of the tidal cycle. This parameter varies around the coastline, with the majority of the toe of the cliffs (6 out of 10 sites) undergoing regular inundation. The beach levels are extracted from the LiDAR data and therefore represent an average between two points in time. It is important to note however, that these levels are subject to seasonal variation and the beach slopes and beach/cliff junction elevations can change according to the wave climate by several meters (Ridgewell and Walkden 2009).

Some preliminary inferences can be drawn from Fig. 5. For example, sites with higher GSI values appear to be more resistant to erosion: Porthcumo has a GSI of 70–75 and a 0.01 m yr⁻¹ rate of erosion, whereas Church Cove has a GSI of 30–35 and an erosion rate of 0.29 m yr⁻¹. However, there are also regions where low rates of erosion are apparent in cliffs with a low rock mass strength: Pendower has a GSI value of 37–40, yet a relatively low erosion rate of 0.01 m yr⁻¹. Clearly, other variables are influential, for example, wave exposure parameterised by H_s and the protection afforded to the cliff toe due to the elevation of the beach (Z_o).

Erosion rates identified in this study are not only a function of the boundary conditions and wave forcing, but also the scale at which the data are captured. The variables that are investigated and the associated scale at which they occur have strong bearing on the results (Naylor et al. 2010). The two most active areas detected in the LiDAR data (Church Cove and Caca Stull Zawn), characterised by erosion rates of 0.2–0.4 m yr⁻¹, are related to the presence of very localised regions of structural weakness or faults. Therefore, the associated erosion rates are perhaps not representative of the stretch of coastline as a whole. For the purposes of statistical analysis, these two sites have been removed to ensure the correlations represent the changes occurring due to processes such as abrasion, quarrying and erosion due to weathering.

Statistical relationships

It is important to consider the relationships between the various boundary conditions and forcing factors at each site to understand what is causing failure on a local scale. The correlation coefficients (r values) between the various parameters and cliff erosion rates allows for these relationships to be drawn. These results are calculated by removing any relationships that have a p value of <0.05, meaning only those that reject the null hypothesis (no linear relationship exists) are considered (Table 4). Although this is a relatively small data set, correlations are apparent between the rates of retreat and the variables acting to control them.

Cliff height is generally considered to play a significant role in the rate of erosion (e.g., along the south coast of the UK; Pethick 1984); yet, some studies have proved cliff height to be a poor predictor of cliff retreat (Dornbusch and Robinson 2005). The fact that both the highest and the lowest rates of retreat are found in cliffs of the same average height (20–25 m) emphasises how this variable tends to be influenced by the rock mass structure that controls the failure mechanisms of the cliffs rather than the height of the cliff itself.

The highest r values between the variables and the rates of retreat were found between the significant wave height (H_s) (0.78) the 10 % exceedance wave height (H_{10}) (0.76), the GSI values (–0.66), and the ratio of the GSI to the significant wave height (–0.77) (Fig. 6).

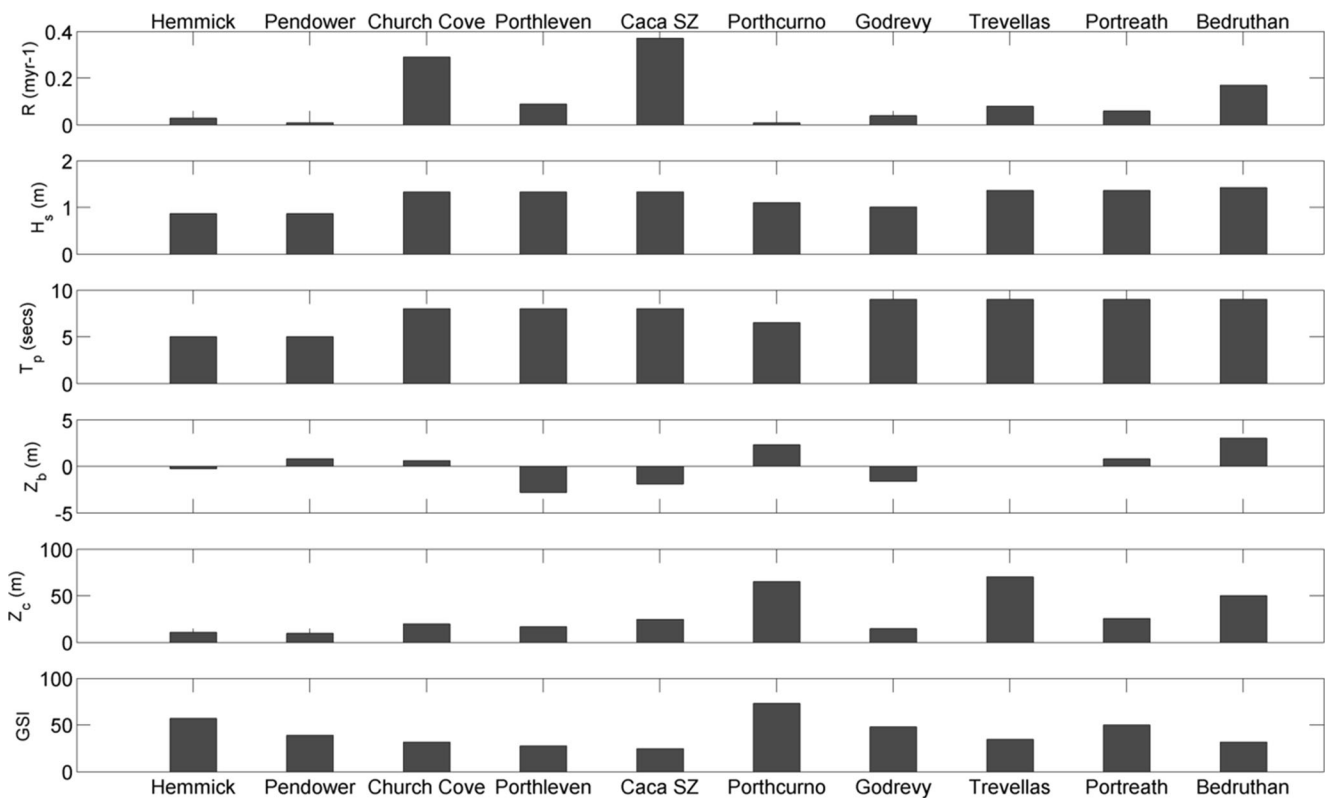


Fig. 5 Rates of retreat, mean H_s , mean T_p , toe exposure (elevation of beach level above/below MHWs (Z_o)), cliff height (Z_c) and GSI at each site. Wave statistics are taken from nearest SWAN output node locations, representative of the regional wave climate

The high r -value (-0.77) for rate of retreat and a simplified version of Sunamura’s rock coast evolution model (Eq. 1b) supports the notion that the ratio of the rock strength to the wave exposure is highly influential in the rate of erosion.

Figure 5 illustrates a number of variables that influence and control hard rock cliff dynamics. It is unlikely that any one factor on its own explains the cliff behaviour and it is more likely that a combination of the different factors should be considered. This indicates how these relationships can only

really be drawn between failures and processes in the longer term. Directly linking large scale failures and forcing would require more detailed, perhaps even in situ, investigations of the variables at a particularly vulnerable site.

Comparison with existing rates of retreat

One of the aims of this study was to compare the rates derived using LiDAR data with the rates used in shoreline management (Table 5) and evaluate whether LiDAR data can be used as a suitable tool to estimate longer term rates of retreat. The rates derived from historic maps and the LiDAR rates tend to agree on the whole. There are regions, however, where large failures have occurred during the time period of the LiDAR study causing the LiDAR-obtained average retreat rates to be close to the upper bound of the range of the longer term recession rates (e.g., at Church Cove, Porthleven and Caca Stull Zawn). Likewise, there are regions where the rate of retreat is much lower than that detected using historic maps, perhaps due to the time constraint of using a relatively modern technology, when only a shorter time period of data are available (e.g., Godrevy and Portreath). Larger scale failures are not detected during this time meaning that an epoch of a few years may not be sufficient. Rates of retreat may be too slow to be captured using historic maps, and not accounted for within the existing rates of retreat. LiDAR data is however

Table 4 r values for correlations between rate of retreat and variables of significant wave height (H_s), the 10 % exceedance wave height (H_{10}), peak spectral wave period (T_p), the elevation of the beach relative to the cliff (Z_o), the cliff height (Z_c), the Geological Strength Index (GSI), and a simplification of Sunamura’s ratio ($GSI:H_s$)

Variable	Correlation coefficient (r value) of variable to rate of retreat (removing Caca Stull Zawn and church cove)
H_s	0.78
H_{10}	0.76
T_p	0.64
Z_o	-0.40
Z_c	0.29
GSI	-0.66
GSI/H_s	-0.77

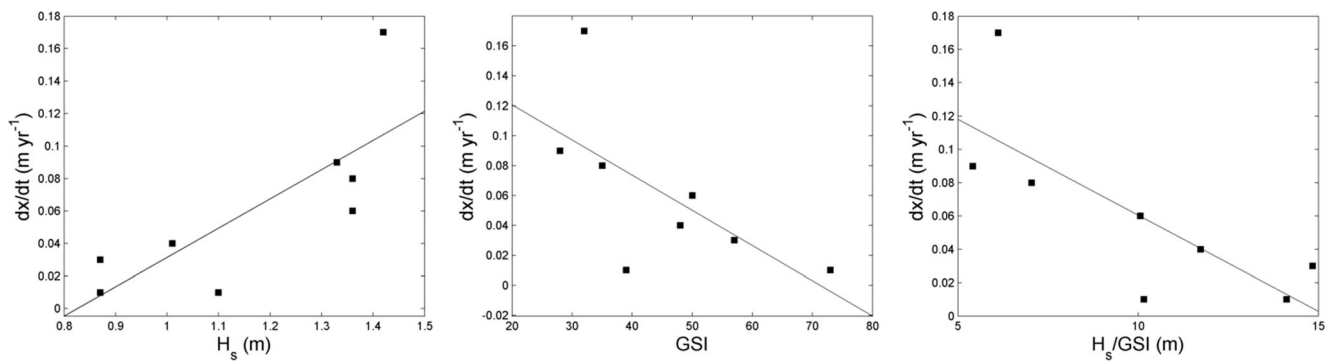


Fig. 6 Relationship between rates of retreat and significant wave height (H_s), GSI and the ratio H_s :GSI. These three plots represent some of the strongest correlations between the variables and observed recession

able to provide recession data in regions that are not identified in large scale coastal behaviour analyses (Hemmick and Bedruthan Steps).

The uncertainty of the recession rates associated with the SMP2 method (indicated with a range of values for each site) is decreased with the LiDAR method as the rate of change to the cliff face over a period of time can be accurately quantified with some degree of certainty (Earlie et al. 2013). These retreat rates differ slightly to those derived in Earlie et al. 2013 as a higher threshold of error was used in this study, to derive more robust erosion rates and eliminate any data that may be attribute to error (Zhang et al. 2005).

The processes involved in the evolution of rocky coastlines are not entirely captured with current methods used for shoreline management purposes. Casting a line along the top of the cliff to represent change does not wholly capture the three dimensional detail of the important changes occurring to the face of the cliff which contribute to overall failure. LiDAR data is a means of obtaining large scale, high resolution geospatial data sets and can be used to accurately and confidently quantify rocky coast evolution for the purposes of

Table 5 Comparison of recession rates derived in this study, using airborne LiDAR with the existing rates of retreat used for shoreline management (SMP2 rates)

Site	SMP2 (historic rate (m yr ⁻¹))	LiDAR method (m yr ⁻¹)
Hemmick	n/a	0.03
Pendower	0.02	0.00
Church cove	0.15–0.25	0.29
Porthleven	0.10–0.25	0.09
Caca Stull Zawn		0.37
Porthcurno	0–0.10	0.00
Godrevy	0.10–0.50 0.02–0.06 Shail and Coggan (2010)	0.04
Portreath	0.40–0.50	0.06
Trevellas	0–0.02	0.08
Bedruthan Steps	n/a	0.17

informing coastal management coastal conservation policies and practices.

Conclusion

In this study we have tested the suitability of using Airborne LiDAR to determine volumetric changes to the cliff face and calculate linear rates of retreat for a slowly eroding geologically ‘resistant’ coastline exposed to a highly energetic wave climate.

DEMs of difference provide volumetric change information for a variety of cliff geometries and allow for not only frequency distributions of failure but also cross-sectional detail on the types of failure mechanisms occurring. Rates of retreat around the Cornish coastline range from 0.01–0.37 m yr⁻¹ and were found to vary according to the spatially varying boundary conditions (rock mass characteristics, beach elevation/ cliff toe exposure) and forcing parameters (significant wave height and peak wave period). The strongest correlations were apparent between the rate of retreat and the significant wave height (H_s) (0.78) and 10 % exceedance wave height (H_{10}) (0.76) and the ratio between the rock mass strength and H_s (0.77).

It is well understood that the accuracy of LiDAR decreases with an increasing slope angle (Adams and Chandler 2002); however, the sensitivity analysis carried out here and by Earlie et al. (2013) shows that even if vertical changes in excess of 0.5 m are disregarded, this has a limited effect on the computed recession rates.

The rates of retreat determined using LiDAR data reflect the long term rates developed in the SMP, yet has highlighted here the level of additional detail the LiDAR method is able to provide. This method has indicated that localised studies are vital to obtaining a more accurate understanding of the rates of erosion on a shorter time scale, especially in hard rock coastlines where failure can be episodic. In terms of understanding hard rock cliff erosion, this study has emphasised the

complexity of these coastal systems. The variety of factors that influence the rates of erosion means there is no single factor causing cliff erosion; the whole system of the physical interactions must be considered holistically in order to understand their evolution.

Acknowledgments The work described in this publication was supported by the European Social Fund Combined Universities in Cornwall Studentship project number 11200NC05. The author would like to thank the National Trust and the Channel Coastal Observatory for information and data provided.

References

- Adams JC, Chandler JH (2002) Evaluation of LiDAR and medium scale photogrammetry for detecting soft-cliff coastal change. *Photogramm Rec* 17:405–418
- Adams PN, Storlazzi CD, Anderson RS (2005) Nearshore wave-induced cyclical flexing of sea cliffs. *J Geophys Res* 110
- Ashton AD, Walkden MJA, Dickson ME (2011) Equilibrium responses of cliffed coasts to changes in the rate of sea level rise. *Mar Geol* 284:217–229
- Austin, M. J., Scott, T. M., Russell, P. E., Masselink, G., 2013. Rip current prediction: development, validation, and evaluation of an operational tool. *Journal of Coastal Research*
- Bird, E. C. F., 1998. *The Coasts of Cornwall: Scenery and Geology with an Excursion Guide*. Alexander Associates
- Brock JC, Purkis SJ (2009) The emerging role of LiDAR remote sensing in coastal research and resource management. *J Coast Res Spec Issue* 53:1–5
- Brooks SM, Spencer T (2010) Temporal and spatial variations in recession rates and sediment release from soft rock cliffs, Suffolk coast, UK. *Geomorphology* 124:26–41
- Brooks SM, Spencer T, Boreham S (2012) Deriving mechanisms and thresholds for cliff retreat in soft-rock cliffs under changing climates: rapidly retreating cliffs of the Suffolk coast, UK. *Geomorphology* 153–154:48–60
- CCO, 2012. Channel Coastal Observatory, Map viewer and data catalogue. Retrieved 01/01/2012, from http://www.channelcoast.org/data_management/online_data_catalogue/
- Cosgrove ARP, Bennett MR, Doyle P (1998) The rate and distribution of coastal cliff erosion in England: a cause for concern? In: Bennett MR, Doyle P (eds) *Issues in environmental geology: a British perspective*. The Geological Society, London
- Damgaard JS, Dong P (2004) Soft cliff recession under oblique waves: physical model tests. *J Waterw Port Coast Ocean Eng* 130:234–242
- Dawson RJ, Dickson ME, Nicholls RJ, Hall JW, Walkden MJA, Stansby PK, Mokrech M, Richards J, Zhou J, Milligan J, Jordan A, Pearson S, Rees J, Bates PD, Koukoulas S, Watkinson AR (2009) Integrated analysis of risks of coastal flooding and cliff erosion under scenarios of long term change. *Clim Chang* 95:249–288
- Dewez TJB, Rohmer J, Regard V, Cnudde C (2013) Probabilistic coastal cliff collapse hazard from repeated terrestrial laser surveys: case study from Mesnil Val (Normandy, northern France). In: Conley DC, Masselink G, Russell PE, O'Hare TJ (eds) *Proceedings 12th international coastal symposium (Plymouth, England)*, journal of coastal research, vol 65, Special Issue No., pp 702–707
- Dickson ME, Pentney R (2012) Micro-seismic measurements of cliff motion under wave impact and implications for the development of near-horizontal shore platforms. *Geomorphology* 151–152:27–38
- Dong P, Guzzetti F (2005) Frequency-size statistics of coastal soft-cliff erosion. *Ocean Eng* 131:37–42
- Dornbusch, U. and Robinson, D., 2005, Controls on chalk cliff erosion in the eastern channel. BAR Phase 1 report, University of Sussex
- Earlie C, Masselink G, Russell P, Shail R (2013) *Proceedings 12th International Coastal Symposium*. In: Conley DC, Masselink G, Russell PE, O'Hare TJ (eds) *J Coast Res. Special Issue No. 65*, Plymouth, England, pp 470–475
- ESRI, 2011. Mapping and analysis for understanding our world. Retrieved 01/03/2012, from <http://www.esri.com/software/arcgis/index.html>
- Geomatics Group, 2012. Geomatics Group; Integrated spatial data. Retrieved 01/02/2012, from <https://www.geomatics-group.co.uk/geocms/>
- Hall JW, Meadowcroft IC, Lee ME, van Gelder PHAJM (2002) Stochastic simulation of episodic soft coastal cliff recession. *Coast Eng* 46:159–174
- Hladik C, Alber M (2012) Accuracy assessment and correction of a LIDAR-derived salt marsh digital elevation model. *Remote Sens Environ* 121:224–235
- Hoek E, Marinov P, Benissi M (1998) Applicability of the Geological Strength Index (GSI) classification for very weak and sheared rock masses. The case of the Athens Schist Formation. *Bull Eng Geol Environ* 57:151–160
- Jaboyedoff M, Oppikofer T, Abellan A, Derron MH, Loye A, Metzger R, Pedrazzini A (2012) Use of LIDAR in landslide investigations: a review. *Nat Hazards* 61:5–28
- Kidner DB, Thomas M, Leight C, Oliver R, Morgan C (2004) Coastal monitoring with LiDAR: Challenges, problems and pitfalls. *Remote Sensing for Environmental Monitoring, Gis Applications, and Geology Iv*. Edited by M. Ehlers, F. Posa, H. J. Kaufmann, U. Michel and G. DeCarolis. Bellingham Spie-Int Soc Opt Eng 5574: 80–89
- Lee EM (2008) Coastal cliff behaviour: observations on the relationship between beach levels and recession rates. *Geomorphology* 101:558–571
- Leigh CL, Kidner DB, Thomas MC (2009) The use of LiDAR in digital surface modelling: issues and errors. *Trans GIS* 13:345–361
- Leveridge B, Hartley AJ (2006) The Variscan Orogeny: the development and deformation of Devonian/Carboniferous basins in SW England and South Wales. In: Brenchley PJ, Rawson PF (eds) *The Geology of England and Wales*. Geological Society of London, London, pp 225–255
- Leveridge BE, Shail RK (2011) The Gramscatho basin, south Cornwall, UK: Devonian active margin successions. *Proc Geol Assoc* 122: 568–615
- Lim M, Rosser NJ, Allison RJ, Petley DN (2010) Erosional processes in the hard rock coastal cliffs at Staithes, North Yorkshire. *Geomorphology* 114:12–21
- Lim M, Rosser NJ, Petley DN, Keen M (2011) Quantifying the controls and influence of tide and wave impacts on coastal rock cliff erosion. *J Coast Res* 27:46–56
- Met Office, 2012. South-west England: Climate. Retrieved 01/09/2012, from <http://www.metoffice.gov.uk/climate/uk/sw/print.html>
- Naylor L, Stephenson W, Trenhaile AS (2010) Rock coast geomorphology: recent advances and future research directions. *Geomorphology* 114:3–11
- Nunes, M., Ferreira, O., Loureiro, C. and Baily, B., 2011. Beach and cliff retreat induced by storm groups at Forte Novo, Algarve (Portugal). *Journal of Coastal Research*, (SI 64), 795–799
- Orford, J., Burgess, K., Dyer, K., Townend, I. and Balson, P. 2002, 'FUTURECOAST – The Integration of Knowledge to Assess Future Coastal Evolution at a National Scale' Paper presented at 28th International Conference on Coastal Engineering, Cardiff, pp. 3221–3233
- Pethick J (1984) *An introduction to coastal geomorphology*. Arnold, London

- Pethick JS, Crooks S (2000) Development of a coastal vulnerability index: a geomorphological perspective. *Environ Conserv* 27:35–367
- Ridgewell J, Walkden M (2009) Cornwall and Isles of Scilly SMP2 Sub-cells review of coastal processes and geomorphology. Royal Haskoning Ltd, Peterborough
- Rogers J, Baptiste A, Jeans K (2009) Proceedings of the 44th flood and coastal risk management conference. UK, Telford, National Coastal Erosion Risk Mapping – The final furlong
- Rosser NJ, Petley DN, Lim M, Dunning SA, Allison RJ (2005) Terrestrial laser scanning for monitoring the process of hard rock coastal cliff erosion. *Q J Eng Geol Hydrogeol* 38:363–375
- Rosser N, Lim M, Petley D, Dunning S, Allison R (2007) Patterns of precursory rockfall prior to slope failure. *J Geophys Res Earth Surf* 112
- Sallenger AH Jr, Krabill WB, Swift RN, Brock J, List J, Hansen M, Holman RA, Manizade S, Sontag J, Meredith A, Morgan K, Yunkel JK, Frederick EB, Stockdon H (2003) Evaluation of Airborne Topographic LiDAR for quantifying beach changes. *J Coast Res* 19:125–133
- Schmidt KA, Hadley BC, Wijekoon N (2011) Vertical accuracy and use of topographic LIDAR data in coastal marshes. *J Coast Res* 27:116–132
- Scott T, Masselink G, Russell P (2011) Morphodynamic characteristics and classification of beaches in England and Wales. *Mar Geol* 286: 1–20
- Shail RK, Coggan JS (2010) Godrevy coastal recession baseline survey 2009–2010. University of Exeter, Camborne School of Mines
- Shail, R., Coggan, J., and Stead, D., 1998. Coastal landsliding in Cornwall, UK: Mechanisms, modelling and implications. Proceedings of the eighth International Congress of the International Association for Engineering Geology and the Environment, (Vancouver, Canada), 1323 – 1330
- Stephenson WJ (2006) Coastal geomorphology. *Prog Phys Geogr* 30: 122–132
- Sunamura T (1992) *Geomorphology of Rocky Coasts*. John Wiley and Sons Ltd., Chichester
- UKHO, 2012. UK Hydrographic Office; Products and Services. Available online at: <http://www.ukho.gov.uk/ProductsandServices/Pages/Home.aspx>. (Accessed: 01/03/2012 2012)
- USGS. 2012. Digital Shoreline Analysis System. Available online at: <http://woodshole.er.usgs.gov/project-pages/dsas/> (Accessed: 01/04/2012 2012)
- Westgate BM, Coggan JS, Pine RJ (2003) Development of a risk-based approach to coastal slope instability assessment in Cornwall. *Geosci south-west England* 10:390–396
- Wood JD, Fisher PF (1993) Assessing interpolation accuracy in elevation models. *Comput Graph Appl IEEE* 13:48–56
- Wyllie DC, Mah CW (2004) *Rock slope engineering: civil and mining*, 4th edn. Spon Press, London
- Xhardé, R., Long, B. F., and Forbes, D. L., 2006. Accuracy and limitations of airborne LiDAR surveys in coastal environments. In 2006 International Geoscience and Remote Sensing Symposium pp. 2412–2415. Denver, CO: IEEE
- Young AP, Ashford SA (2006) Application of airborne LIDAR for seacliff volumetric change and beach-sediment budget contributions. *J Coast Res* 22:307–318
- Young AP, Flick RE, Gutierrez R, Guza RT (2009) Comparison of short-term seacliff retreat measurement methods in Del Mar, California. *Geomorphology* 112:318–323
- Young AP, Guza RT, O’Reilly WC, Flick RE, Gutierrez R (2011a) Short-term retreat statistics of a slowly eroding coastal cliff. *Nat Hazards Earth Syst Sci* 11:205–217
- Young AP, Adams P, O’Reilly WC, Flick RE, Guza RT (2011b) Coastal cliff ground motions from local ocean swell and infragravity waves in southern California. *J Geophys Res* 116
- Zhang K, Whitman D, Leatherman S, Robertson W (2005) Quantification of beach changes caused by hurricane Floyd along Florida’s Atlantic coast using airborne laser surveys. *J Coast Res* 21:123–134